Effects of Secondary Structure on DNA and RNA Cleavage by Diplatinum(II)†

Pamela J. Carter, Klaus M. Breiner, and H. Holden Thorp*

Department of Chemistry, University of North Carolina, Chapel Hill, North Carolina 27599-3290

Received June 23, 1998; Revised Manuscript Received August 4, 1998

ABSTRACT: The photochemistry of $Pt_2(pop)_4^{4-}$ with nucleic acids has been studied using radiolabeled oligomers of DNA and RNA and high-resolution electrophoresis (pop is $P_2O_5H_2^{2-}$). Photolysis of $Pt_2(pop)_4^{4-}$ with duplex DNA produces an even cleavage ladder and relatively little enhancement of cleavage upon treatment with piperidine. In contrast, the cleavage pattern is far less regular with single-stranded DNA, and there is a large enhancement in cleavage upon treatment with piperidine. Accordingly, photolysis of $Pt_2(pop)_4^{4-}$ with the DNA hairpin 5′-d[ATCCTATTTATAGGAT] produces a much larger piperidine enhancement at the loop and end nucleotides than in the stem. There is an additional piperidine enhancement that occurs selectively at guanine residues either in RNA or in DNA at low Mg^{2+} concentrations that is attributed to outer-sphere electron transfer on the basis of the known excited-state redox potentials of $Pt_2(pop)_4^{4-*}$ and the expected oxidative chemistry of guanine. The extent of guanine oxidation is higher compared to the extent of sugar oxidation at low Mg^{2+} concentrations, which can be attributed to a shallower distance dependence for electron transfer compared to that for atom transfer. The effects of Mg^{2+} and piperidine or aniline treatment were examined on stem−loop structures of DNA and RNA and gave partial images of the expected secondary structures.

The availability of combinatorial selection strategies for nucleic acids has led to the rapid proliferation of diverse DNA and RNA structures with a wide range of physiological and catalytic activities (*1*, *2*). As a result, assessing structural features of noncanonical DNAs, RNAs, and their protein complexes rapidly and on small quantities of material has become increasingly important. Determining the reactivity of individual nucleotides in a complex nucleic acid toward enzyme or chemical nucleases is an attractive approach because only quantities sufficient for radiolabeling are required. For example, some enzyme nucleases cleave either DNA or RNA only at single-stranded sites and usually for a specific base. Similarly, some chemical nucleases oxidize guanine preferentially at single-stranded sites (*3*−*6*). An unrealized goal in this area is a chemical means for selectively cleaving single-stranded regions in DNA and RNA by sugar oxidation, where no base preference is observed. Such a method would allow for mapping the secondary structure of a complex DNA or RNA in a single cleavage reaction. Realization of this goal will require an understanding of the effects of the secondary structure not only on the efficiency of formation of the primary lesion but also on any followup reactions required to produce strand scission. We report here on progress toward these goals made through studies of a photocleavage reaction that illustrates the importance of the secondary structure in dictating the relative reaction rates of cleavage at different nucleotides.

The excited state of $Pt_2(pop)_4^{4-}$ is reactive toward hydrogen atom abstraction and both reductive and oxidative electron transfer (pop is $P_2O_5H_2^{2-}$) (*7*). The complex abstracts hydrogen atoms from a wide range of substrates, including alcohols, hydrocarbons, silanes, and stannanes. For example, the quenching rate constant for abstraction of hydrogen atom from diphenylmethanol is $2 \times 10^5\ M^{-1}\ s^{-1}$. The complex is quenched by electron donors such as aromatic amines and very efficiently by electron acceptors such as pyridiniums and viologens. Thus, $Pt_2(pop)_4^{4-}$ is a powerful excited-state reductant and a modest excited-state oxidant. We have described previously the fact that $Pt_2(pop)_4^{4-}$ cleaves duplex DNA upon photolysis by abstraction of both the 4′- and 5′-hydrogens of the 2′-deoxyribose moiety in an excited-state atom transfer reaction (*8*). We report here on the possibility of excited-state electron transfer reactivity in the photochemistry of $Pt_2(pop)_4^{4-}$ with DNA.

The partitioning between electron and atom transfer reactions has been an important issue in recent studies of DNA modification. For example, Schuster and co-workers (*9*) have shown that anthraquinone derivatives cleave DNA by atom transfer when bound to the outside of DNA near the sugar−phosphate backbone but by electron transfer from guanine when intercalated into the base stack. Similarly, complexes based on $Rh(phen)_2(phi)^{3+}$ cleave DNA by atom transfer upon high-energy irradiation but by electron transfer from guanine upon low-energy irradiation (*10*). Coordinatively unsaturated nickel complexes catalyze the inner-sphere oxidation of guanine by persulfate via a pathway where covalent binding of nickel to guanine provides selectivity for distorted and single-stranded guanine sites (*5*). When no distorted guanines sites are present, however, there is evidence for oxidation of guanine by outer-sphere electron transfer at relatively long range (*11*). These observations point to a model where the outer-sphere guanine reaction is

† This work was supported by the National Science Foundation. H.H.T. acknowledges the support of a Camille Dreyfus Teacher-Scholar Award and an Alfred P. Sloan Fellowship.

S0006-2960(98)01479-2 CCC: $15.00
Published on Web 09/02/1998

always a potential competitor for inner-sphere atom transfer reactions of DNA modification agents. Observation of the outer-sphere reaction is generally limited to cases where the atom transfer reaction has been impeded because of poor proximity of the oxidant to the reactive site or energetically discouraged because of the irradiation wavelength. Because the distance dependence for electron transfer reactions is relatively shallow compared to that for atom transfer reactions, favorable association of the oxidant is not required to achieve a finite rate constant.

We report here that atom transfer from single-stranded DNA to $Pt_2(pop)_4^{4-}$* gives a piperidine enhancement that is not observed when the same strand is hybridized to its complement. This enhancement is also evident in the single-stranded regions of hairpin DNAs. In explaining the secondary structure effect, differences in the rates of formation of the primary lesion or in the followup chemistry that leads to strand scission must be considered. We also find evidence for an electron transfer reaction where $Pt_2(pop)_4^{4-}$* acts as an excited-state oxidant of guanine to produce an alkali-labile lesion. This electron transfer reaction is only competitive with sugar oxidation in DNA at low Mg^{2+} concentrations where there is poor association with the sugar−phosphate backbone or in RNA where the sugar hydrogens are considerably less reactive than in DNA. The dependence of the relative efficiencies of the atom transfer and oxidative electron transfer reactions on Mg^{2+} concentration, base treatment, and secondary structure provides a consistent picture of competition between the various oxidation pathways.

MATERIALS AND METHODS

Metal Complex. $K_4[Pt_2(pop)_4]$ was prepared by a literature method (*12*). Aqueous stock solutions were frozen in small aliquots, and the concentration was determined by UV absorbance [$\epsilon_{367nm} = 34\,500\ M^{-1}\ cm^{-1}$ (*12*)].

Preparation and Labeling of DNA Oligomers. All DNA and RNA concentrations throughout are given per strand of oligonucleotide. All DNA oligomers were acquired from the Oligonucleotide Synthesis Center in the Department of Pathology at the University of North Carolina and were purified by HPLC using a 15 cm column packed with SelfPack Poros 20 R2 (PerSeptive Biosystems) with a 0 to 20% gradient (buffer A, 50 mM triethylammonium acetate and 5% acetonitrile; and buffer B, 100% acetonitrile). The collected solutions were lyophilized to near dryness and twice precipitated with ethanol. The oligonucleotides were resuspended in MilliQ water, and concentrations were determined by UV absorbance, as described elsewhere (*13*). Portions used for end labeling were additionally purified on a 20% polyacrylamide gel, visualized by UV shadowing, and extracted from the gel, as described elsewhere (*3*). The 5′-^{32}P-labeled oligomer was prepared using T4 polynucleotide kinase (New England Biolabs) and 2′-deoxyadenosine 5′-[γ-^{32}P]triphosphate (Amersham) as previously described (*14*). Hairpin sequences were heated to 80 °C and then chilled quickly to room temperature in a water bath to avoid formation of bulge complexes. Hairpin formation was confirmed by running the samples on a 20% nondenaturing polyacrylamide gel at 4 °C. The folded hairpins gave a single band by native gel electrophoresis.

Chart 1

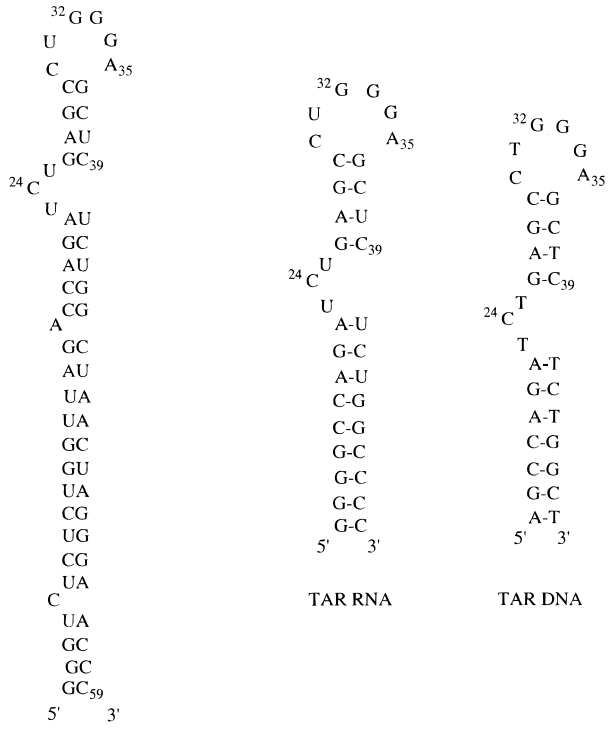

DNA Photocleavage Reactions. Photolysis was performed in polyspring inserts (Fisher Scientific Co.) with a 300 W Hg lamp (Oriel) and a monochromator providing 368 nm (60% transmission, 40 nm fwhm) light. Typical final concentrations were 5−8 μM DNA, 10 mM sodium phosphate buffer (pH 7.0), 5 mM $MgSO_4$, and 25 μM $K_4[Pt_2(pop)_4]$. The total volumes per reaction were 40 μL, and the irradiation time was 10 min. Other specific reaction conditions are given in the figure legends. After photolysis of the DNA/$Pt_2(pop)_4^{4-}$ samples, 1 μg of phenol/chloroform-purified calf thymus DNA, 10 μL of 1 M KCN, and 10 μL of 0.2 M EDTA were added. The mixtures were then incubated at 50 °C for 30 min to remove covalently attached Pt(II) resulting from the decomposition of $Pt_2(pop)_4^{4-}$ during photolysis. Ethanol precipitation, alkaline treatment with piperidine, and loading procedures were carried out as described elsewhere (*14*). The DNA fragments were analyzed using 20% polyacrylamide (19:1 acrylamide/bisacrylamide) gel electrophoresis under denaturing conditions (7 M urea). Cleavage bands were visualized using Kodak BioMax MR film, which was exposed at −78 °C for 10−24 h. The extent of cleavage was quantitated using an Apple OneScanner and the NIH Image program. Care was taken to ensure that saturation of the film did not occur and that densitometry gave Gaussian peaks for all bands denoted in the histograms.

Preparation and Labeling of the RNA Oligomer. A truncated analogue of the HIV-1 TAR RNA (Chart 1) was prepared by in vitro transcription using T7 RNA polymerase and a synthetic DNA template (*15*). Extra G's were incorporated at the 5′-end to increase the efficiency of transcription. The template strand was annealed to the T7 promoter strand (5′-TAATACGACTCACTATAG) in 10 mM sodium phosphate buffer by heating to 90 °C for 5 min and cooling slowly for 1 h. The transcription reaction was

then carried out in 40 mM Tris-HCl (pH 8.0), 15 mM $MgCl_2$, 5 mM DTT, 2 μg of BSA, and 2.0 mM NTPs at 37 °C for 3 h. For every picomole of template DNA, 5 units of T7 RNA polymerase (Amersham) was used. To minimize enzymatic degradation of the RNA, 1 μL of RNasin (Promega) (30 units/μL) was added to the transcription reaction mixture. The RNA was purified on a 20% polyacrylamide denaturing (7 M urea) gel, visualized by UV shadowing, and isolated from the gel as described above. To elute the RNA from the gel slice, an extraction buffer containing 0.5 mM ammonium acetate, 0.1% SDS, and 0.1 mM EDTA (pH 7.8) was used. The RNA was 3′-end labeled with T4 RNA Ligase (New England Biolabs) and cytidine 3′,5′-[5′-^{32}P]biphosphate (Amersham) by incubating at 4 °C for 10−12 h (*16*). The labeled RNA was purified on a 20% polyacrylamide denaturing gel in a similar manner as described above, and the RNA samples were stored in DEPC-treated water at −20 °C.

RNA Photocleavage Reactions. A solution consisting of 3′-labeled RNA (27 nCi), sodium phosphate buffer (pH 7.0), and carrier tRNA (0.28 μg/μL) was transferred into the polyspring inserts. An aliquot (10 μL) of the solution containing $Pt_2(pop)_4^{4-}$ and $MgSO_4$ was then added, making the final reaction volume 20 μL. The solutions were stirred carefully with a pipet tip and photolyzed for 30 min. Typical final concentrations were ~1 μM RNA (including the carrier tRNA), 10 mM sodium phosphate buffer (pH 7.0), 2 mM $MgCl_2$, and 400 μM $K_4[Pt_2(pop)_4]$. Variations in these concentrations are provided in the figure legends. After photolysis, any covalently bound Pt(II) was removed by addition of 10 μL of 2,3-dimercaptosuccinic acid (pH 7.0) followed by incubation of the mixture at 50 °C for 20 min. The samples were then transferred to RNase-free Centricon filters (Amicon) with a MW cutoff of 3000 and centrifuged for 20 min to remove the majority of any salts. The RNA was then recovered by ethanol precipitation and rinsed once with ethanol to ensure the removal of excess salt. The appropriate samples were aniline treated (1.0 M aniline/acetate buffer at pH 4.5) by a procedure that is described elsewhere (*17*). Electrophoresis and gel analysis were performed as described above for DNA.

RESULTS

Single Strand and Duplex. For duplex DNA where only the 4′- and 5′-hydrogens are abstracted, the majority of cleavage by $Pt_2(pop)_4^{4-}$ is apparent prior to piperidine treatment, although there is a modest piperidine enhancement as expected for the 4′-hydrogen pathway (*18*). To elucidate the effects of hybridization on the available pathways and cleavage efficiency, we studied the cleavage of a single strand d[5′-$A_1T_2G_3C_4C_5C_6T_7T_8G_9C_{10}G_{11}T_{12}A_{13}T_{14}$], which is a random coil in solution (*14*). The results of cleavage of this oligonucleotide both as a single-strand and hybridized to its complement are shown in Figure 1. For the duplex, a relatively even cleavage ladder is observed, as reported previously (*8*). In the single strand, cleavage at every nucleotide is still observed, although the ladder is not as even as that seen with the duplex. Much larger differences between the single strand and duplex are observed following piperidine treatment, which indicates either that there is an additional site of oxidation in the single strand that is not available in the duplex or that the piperidine-dependent pathway is more efficient for single-stranded substrates. As described below, we have evidence for oxidation of guanine, most likely by one-electron transfer producing a piperidine-labile site, which could contribute to the piperidine enhancements observed at guanines (at G11 and G9) in Figure 1 but not to the enhancements observed at the A, T, and C residues.

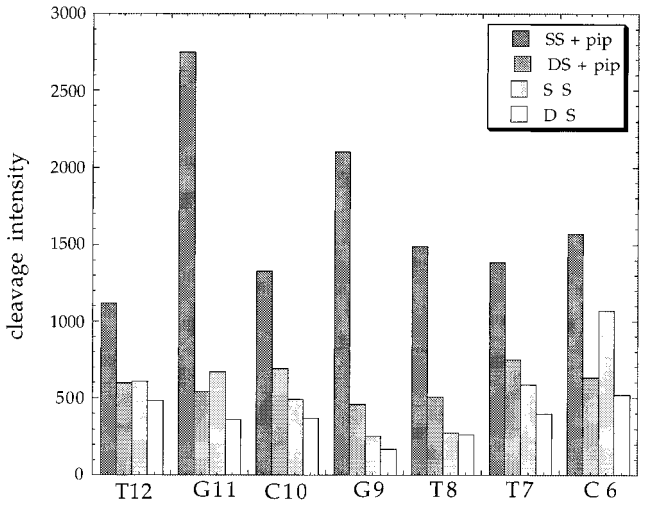

FIGURE 1: Histogram showing the extent of cleavage of 5′-^{32}P-labeled d[5′-$A_1T_2G_3C_4C_5C_6T_7T_8G_9C_{10}G_{11}T_{12}A_{13}T_{14}$] by $Pt_2(pop)_4^{4-}$ [100 μM $Pt_2(pop)_4^{4-}$ and 5 mM $MgSO_4$] hybridized to its complement (DS), as a single strand (SS), hybridized to its complement and treated with piperidine (DS + pip), and as a single strand and treated with piperidine (SS + pip). All conditions and quantitation procedures are given in Materials and Methods. Errors in quantitation of cleavage intensities were ±25% or less throughout the paper.

The larger piperidine enhancement observed for single strands compared to that for duplexes suggested that the piperidine enhancement could be used to map the secondary structure of DNAs containing both single-stranded and duplex regions. For initial studies, we chose to test this hypothesis on a hairpin whose structure had been studied in solution by NMR, d[5′-$A_1T_2C_3C_4T_5A_6$**$T_7T_8T_9A_{10}$**$T_{11}A_{12}$-$G_{13}G_{14}A_{15}T_{16}$] (hairpin loop residues are bold) (*19*). We have used this hairpin previously in studies of cleavage by Ru(tpy)(bpy)O^{2+} (*3*). The NMR structure of the hairpin shows a well-defined duplex stem of six nucleotides with a compact tetraloop where residues T_7 and A_{10} form a Hoogsteen base pair (*19*). The results of photocleavage of this oligonucleotide with $Pt_2(pop)_4^{4-}$ are shown in Figure 2. For the stem region, the expected even ladder is observed prior to piperidine treatment with more variable intensity in the loop region. Upon treatment with piperidine, there is relatively little enhancement in the stem region but much larger average enhancement in the loop. These features are readily apparent in the histogram shown in Figure 3. The largest enhancement is observed at T9, which is pointing out of the loop in the solution structure (*19*). There is also a large enhancement at the end nucleotide (T_{16}), where greater accessibility of the sugar sites is expected.

Excited-State Oxidation of Guanine. Inspection of the results for duplex DNA published previously shows a slightly greater piperidine enhancement at guanine residues (see Figure 1 in ref *8*). As described above, the cleavage agent $Pt_2(pop)_4^{4-}$ undergoes a known quenching reaction with electron donors and should be thermodynamically capable of oxidizing guanine by one electron (*7*, *20*). The Stern−

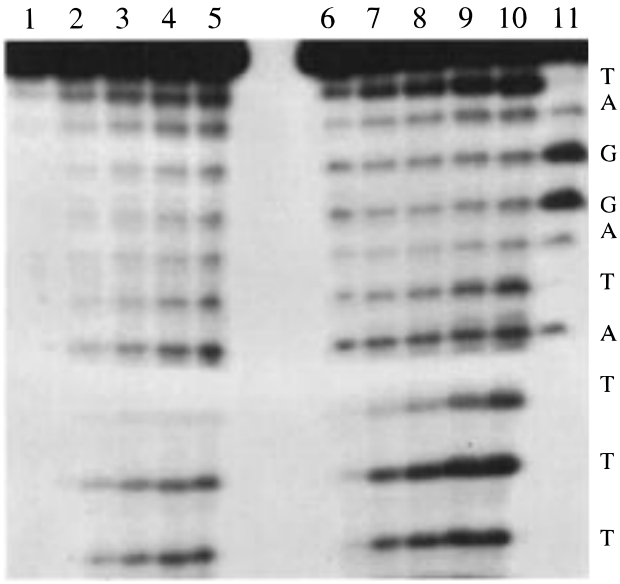

FIGURE 2: Autoradiogram of a polyacrylamide gel showing the reaction of 5′-^{32}P-labeled d[5′-$A_1T_2C_3C_4T_5A_6$**$T_7T_8T_9A_{10}$**$T_{11}A_{12}$-$G_{13}G_{14}A_{15}T_{16}$] with $Pt_2(pop)_4^{4-}$: lanes 1−5, DNA photolyzed with 0, 25, 50, 100, and 200 μM $Pt_2(pop)_4^{4-}$, respectively, and 5 mM $MgSO_4$; and lanes 6−10, lanes 1−5 after piperidine treatment, respectively.

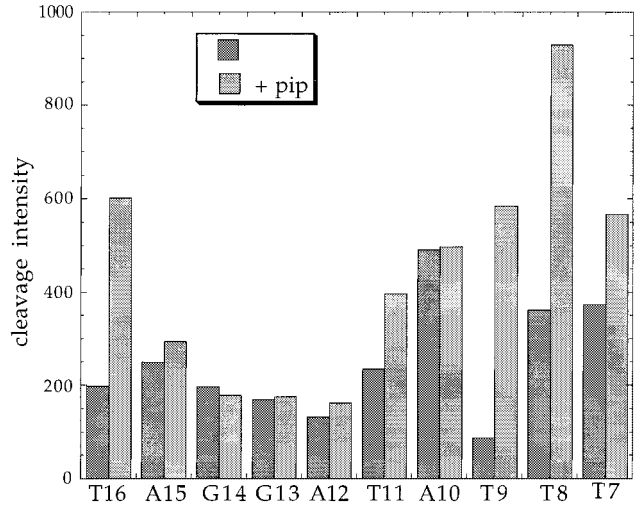

FIGURE 3: Histogram showing the results from Figure 2 with 100 μM $Pt_2(pop)_4^{4-}$ for cleavage with piperidine (+pip) and without piperidine.

Volmer rate constant for oxidation of *N*,*N*-diphenylbenzenamine ($E_{1/2}$ = 0.92 V vs SCE) is 1.5×10^6 M^{-1} s^{-1} (*7*), so oxidation of guanine ($E_{1/2}$ = 1.05 V vs SCE) (*21*) occurs with an intrinsic rate constant of probably about 10^5 M^{-1} s^{-1}, which is similar to that for hydrogen abstraction. Outer-sphere guanine oxidation is therefore likely to compete with hydrogen abstraction in DNA photoreactions. Numerous studies have shown that one-electron oxidation of guanine eventually leads to piperidine-labile cleavages specifically at guanine nucleotides (*10*, *22*−*27*). In the evaluation of the effects of secondary structure on the piperidine enhancement, the side reaction involving guanine oxidation must therefore be considered. In duplex DNA, the guanine residue is buried in the center of the double helix, so in the presence of Mg^{2+} ion, the guanine reaction occurs to a similar or lesser extent than the sugar oxidation. However, in the single strand where the guanine is more solvent-accessible, the guanine electron transfer reaction can compete with sugar oxidation.

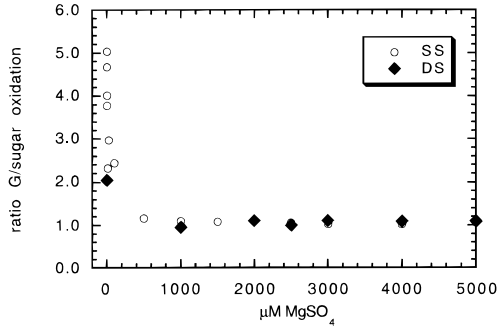

FIGURE 4: Graph showing the effect of Mg^{2+} on the guanine:sugar oxidation ratio for the random coil sequence d[5′-$A_1T_2G_3C_4C_5$-$C_6T_7T_8G_9C_{10}G_{11}T_{12}A_{13}T_{14}$]. The concentration of $Pt_2(pop)_4^{4-}$ was 100 μM for the single-stranded substrate (SS) and 50 μM for the duplex (DS). Piperidine treatment was performed as described in Materials and Methods.

Electron transfer reactions between guanine and nonintercalating reagents occur with a significant but finite distance dependence corresponding to a β of about 1 $Å^{-1}$ (*11*, *28*). In contrast, the atom transfer pathway likely requires much more intimate contact between the reagent and the abstracted hydrogen. Therefore, the sugar reaction is much more efficient in the presence of Mg^{2+} ion, which decreases the electrostatic repulsion and allows for more intimate contact of $Pt_2(pop)_4^{4-*}$ with the sugar−phosphate backbone. Photocleavage with $Pt_2(pop)_4^{4-}$ was carried out for the sequence d[5′-ATGCCCTTGCGTAT] as a single strand and duplex. The extent of guanine and sugar scission after piperidine treatment was quantitated, and Figure 4 shows a plot of the guanine:sugar ratio versus the concentration of Mg^{2+} ion. (We did not attempt to correct for the fact that the cleavage at guanine represents contributions from both the electron transfer and atom transfer pathways.) The guanine:sugar ratio decreases upon addition of Mg^{2+}, which is the expected result if the atom transfer pathway exhibits a steeper distance dependence than the electron transfer pathway. Further, the guanine:sugar ratio for the single-stranded substrate exhibits a much steeper dependence on Mg^{2+} concentration, whereas the duplex shows less Mg^{2+} concentration dependence. In the duplex form, the maximal electron transfer reactivity of guanine toward weakly bound oxidants cannot be realized due to steric protection by the complementary strand, as we and others have discussed in detail for related reactions (*3*, *5*, *28*). Therefore, the maximal guanine:sugar ratio is lower for the duplex form than for the single strand. No piperidine enhancement at guanine was observed in Figures 1 and 2 because these studies were conducted at 5 mM Mg^{2+}.

TAR Sequence. Complete expression of the HIV-1 gene is regulated by binding of a trans-activating factor (tat) to the bulge−loop mRNA sequence known as TAR (*29*−*31*). The secondary structure of TAR mRNA is shown in Chart 1 for both the RNA and a DNA analogue used in these studies and previously in studies of the cleavage chemistry of $Ru(tpy)(bpy)O^{2+}$ (*32*). The bulge−loop motif of the TAR sequence provides an interesting substrate for $Pt_2(pop)_4^{4-}$ because there are two single-stranded regions. In RNA, the atom transfer pathway is considerably slower because the 2′-hydroxyl deactivates the C−H bonds in the sugar, which we have commented on extensively elsewhere (*33*); cleavage

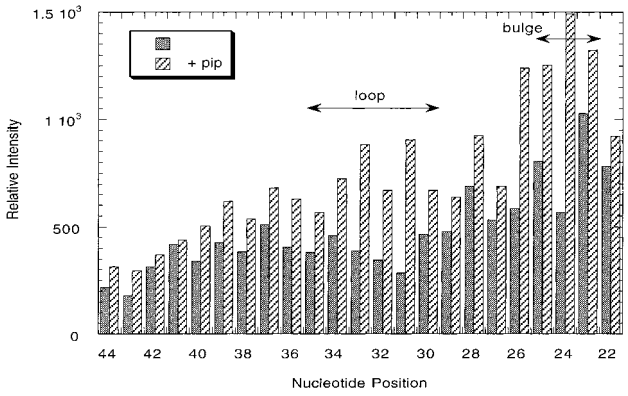

FIGURE 5: Histogram showing the effects of piperidine treatment on TAR DNA. The final concentrations of $Pt_2(pop)_4^{4-}$ and $MgSO_4$ were 100 μM and 5 mM, respectively.

of RNA by $Ru(tpy)(bpy)O^{2+}$ produces almost exclusively guanine oxidation, while both guanine and sugar oxidation are observed in DNA (*32*). We have therefore studied RNA and DNA analogues in parallel, because it is more difficult to visualize the sugar chemistry in the RNA oligomers. The DNA analogue of TAR was studied with enediynes for similar reasons (*34*).

Cleavage of TAR DNA produces an even cleavage ladder prior to piperidine treatment, as shown in Figure 5. Following piperidine treatment, large enhancements are observed in the loop and bulge regions, with the most noticeable enhancement at C24 within the bulge. The large stem region (G36−G44) shows very little piperidine enhancement, even at the nucleotides across from the three-nucleotide bulge. The four nucleotides between the bulge and loop (G26−C29) show variable piperidine enhancement, which is particularly interesting since very little enhancement is seen in the four complementary nucleotides on the other side of the loop (G36−C39). This variability might result from distortion of the side of the duplex that connects the loop and bulge regions.

Decomposition of the metal complex occurs during the photolysis of $Pt_2(pop)_4^{4-}$ and leads to cross-linking of the nucleic acid by liberated platinum. In DNA reactions, the coordinated platinum is removed by treatment with cyanide (*8*). However, CN^- is strong enough as a base to promote hydrolysis of RNA, so we have developed an alternative protocol using 2,3-dimercaptosuccinic acid that is described in detail in Materials and Methods. A relatively even cleavage ladder is produced prior to aniline treatment (Figure 6), and the total aniline enhancement observed in RNA is much greater than the piperidine enhancement observed in DNA. There is perhaps greater aniline enhancement in the loop region; however, there is also significant aniline enhancement at all of the guanine residues. The even cleavage ladder obtained following aniline treatment suggests that high-resolution footprinting of RNA nucleoprotein complexes with $Pt_2(pop)_4^{4-}$ will be feasible.

The aniline enhancement somewhat reflects the secondary structure of the TAR RNA oligomer, although the differences in aniline enhancement at individual nucleotides are much smaller than the differences in piperidine enhancement in DNA. Figure 7 shows a histogram of cleavage intensities before and after treatment with aniline. The secondary structure of the loop region is barely discernible, while the

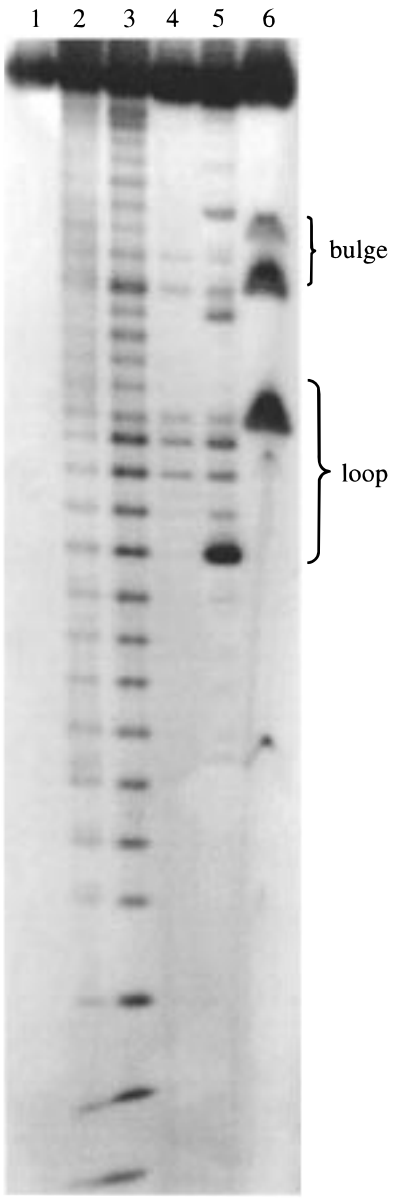

FIGURE 6: Autoradiogram of a poylacrylamide gel showing the reaction of the 3′-^{32}P-labeled TAR RNA analogue: lanes 1 and 2, RNA photolyzed with 0 and 400 μM $Pt_2(pop)_4^{4-}$, respectively, and 2 mM $MgSO_4$; lanes 3 and 4, lanes 2 and 1 with aniline, respectively; and lanes 5 and 6, A (DEPC) and U (hydrazine) lanes, respectively.

bulge region displays no aniline enhancement whatsoever. Large enhancements are observed at the loop guanines (G32, G33, and G34) and probably arise from changes in the secondary structure or from guanine side reactions. Therefore, a general pattern of enhancement at guanine is superimposed over the variations that arise from the secondary structure. The greater degree of guanine oxidation in RNA is probably a result of the decrease in sugar reactivity induced by the 2′-OH. Nevertheless, there is a large aniline enhancement at A35 at the 3′-side of the loop in the TAR RNA after cleavage by $Pt_2(pop)_4^{4-}$.

For duplex DNA, where the abstracted 4′- and 5′-hydrogens reside in the minor groove, photocleavage by $Pt_2(pop)_4^{4-}$ is dramatically enhanced by addition of Mg^{2+}, which alleviates some of the electrostatic repulsion between the ordered phosphates of the minor groove and the tetraan-

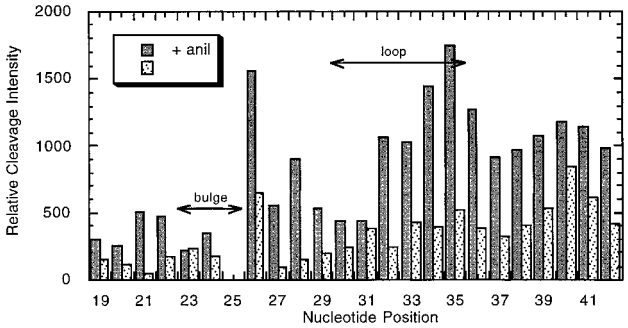

FIGURE 7: Histogram showing the effect of aniline treatment on cleavage of TAR RNA. Raw intensities are shown for the extents of cleavage before and after treatment with aniline; data were taken from Figure 6. The extent of aniline enhancement was a factor of 3 or less.

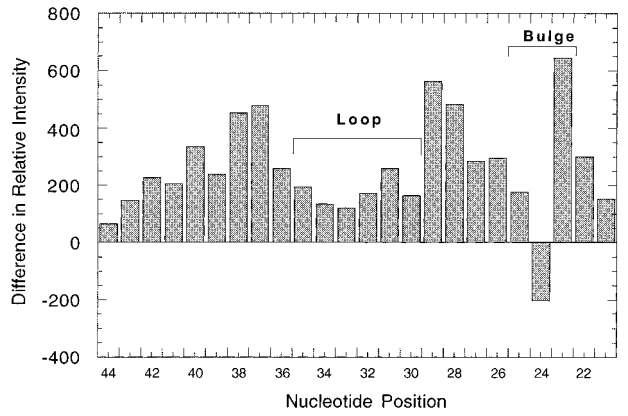

FIGURE 8: Histogram showing the effect of Mg^{2+} (2 mM) on the cleavage of TAR DNA in the absence of piperidine treatment. Enhancements were calculated for each site by subtracting the relative cleavage intensity without added Mg^{2+} from the relative cleavage intensity with added Mg^{2+}. The concentration of $Pt_2(pop)_4^{4-}$ was 100 μM.

ionic complex. Since single-stranded regions do not present such an ordered array of anionic charges, less enhancement of cleavage by Mg^{2+} might be expected. Figure 8 shows the effect of Mg^{2+} on cleavage of the TAR DNA sequence by $Pt_2(pop)_4^{4-}$. This experiment was carried out without any piperidine treatment, so the only cleavage we are observing is from 4′- and 5′-sugar oxidation and not guanine modification. An abrupt decrease in Mg^{2+} enhancement is observed for the residues within the single-stranded loop and includes a guanine residue adjacent to the loop. The enhancement in the bulge region is variable, but easily distinguishable from the stem regions. The central bulge nucleotide C24 is actually protected from oxidation by addition of Mg^{2+}, and we have observed unusual behavior at this nucleotide with other reagents (*32*). A decrease in Mg^{2+} enhancement is also observed at residues G43 and G44, which are near the 3′-end and are probably single-stranded at least part of the time. Like the histogram for aniline enhancement, Figure 8 provides a partial image of the secondary structure of the sequence. The average changes in cleavage intensity as a function of added Mg^{2+} are as follows: loop residues, 70%; duplex residues, 220%; and bulge residues, 180%. These values are in good qualitative agreement with the expected degree of negative charge at each type of site. An advantage of this approach is that changes in the reaction chemistry of the nucleotides will not affect the influence of Mg^{2+} on the cleavage yields, so RNA and DNA behave similarly. A drawback to using Mg^{2+} to image the secondary structure is that complicated structures, particularly those in RNA, are often sensitive to the Mg^{2+} concentration (*35*).

DISCUSSION

Secondary Structure Effects. The activation of the 4′- and 5′-hydrogens by $Pt_2(pop)_4^{4-}$* was readily established on the basis of the observations of the 3′-phosphoglycolate and the 5′-aldehyde on sequencing gels (*8*). Apparently, the primary photoreaction that generates the 4′- and 5′-radicals is sensitive to the ability of $Pt_2(pop)_4^{4-}$* to approach the reactive site. Thus, there is a significant effect of Mg^{2+}, which can reduce the electrostatic repulsion and provide for a closer approach of $Pt_2(pop)_4^{4-}$* to the activated C−H bond. This effect is apparent in the comparison of the atom transfer and electron transfer pathways (Figure 4) where an increased level of binding of the Mg^{2+} ion by duplex DNA increases the efficiency of sugar radical production. The piperidine enhancements suggest that the pathway that produces the piperidine-labile scission is also selective for single-stranded DNA. This effect therefore amplifies the difference in reactivity of single-stranded and duplex sites; therefore, the greatest difference in single-stranded and duplex reactivity is seen when comparing the spontaneous and alkali-labile scission.

As stated above, a probable origin for the secondary structure selectivity is that the relative rates of the primary reactions that form the 4′- and 5′-radicals are different for single strands and duplexes. An alternative explanation is that the piperidine-enhanced cleavage arises from activation of the 1′-C−H in the loop, which is not accessible in the duplex region. This explanation is supported by mononucleotide studies, which indicate that hydrogens other than 4′- and 5′-hydrogens might also be reactive (*36*). Oxidation of the 1′-hydrogen leads to a lesion that produces strand scission mainly after piperidine treatment, so one explanation for the large piperidine enhancement in the single strand is that the 1′-hydrogen is sterically inaccessible in duplex DNA but is available for abstraction in single strands. The 1′-hydrogen resides deep within the minor groove (*37*) and would be accessible only under close contact between the metal complex and the DNA, which is precluded by the anionic charge of the complex. However, previous studies using this TTTA hairpin demonstrated that oxidation by Ru(tpy)(bpy)-O^{2+}, which is energetically capable of oxidizing only the 1′-C−H bond, is generally more prevalent within the loop (*3*), which is consistent with the 1′-site being more accessible. In this earlier study (*3*), the order of reactivity within the loop was as follows: A10 ∼ T8 > T7 ≫ T9. In these studies, the extent of piperidine enhancement falls in a different order where T9 > T8 > T7 ≫ A10. An important caveat here is that there is significant binding for the oxoruthenium(IV) reagent (*38*) and not for $Pt_2(pop)_4^{4-}$, so this observation does not exclude activation of the 1′-site in the loop as an origin for piperidine enhancement. Likewise, oxidation of the methyl group of thymidine is a possibility, although toluene is not a particularly good substrate for $Pt_2(pop)_4^{4-}$* (*7*).

Recently, Schuster and co-workers have reported that an anthraquinone derivative selectively targets the loop region of a DNA hairpin (*25*). In this case, NMR studies show a

binding interaction of the anthraquinone with the loop bases. Since no binding of the $Pt_2(pop)_4^{4-}$ tetraanion to the nucleic acid occurs, the selectivity for the loop reported here must arise either from a greater solvent accessibility of the oxidized site in the loop, a lower electrostatic repulsion of the tetraanion from the single-stranded region, or both. In the anthraquinone case, numerous experiments support the cleavage of nucleotides near the site of binding, so the observed selectivity supports a preference for binding of the hydrophobic anthraquinone near the loop region. Taken together, the two studies suggest that there are multiple mechanisms for targeting hairpin loops by either enhanced binding or greater chemical reactivity.

Guanine Oxidation. The additional alkali-labile scission at guanine observed at low Mg^{2+} concentrations is most likely due to outer-sphere oxidation by $Pt_2(pop)_4^{4-}$*. The excited state is a modest one-electron oxidant; however, inspection of known rate constants for a variety of amine donors suggests that guanine ($E_{1/2} = 1.05$ V vs SCE) should quench $Pt_2(pop)_4^{4-}$* with a rate constant of about 10^5 M^{-1} s^{-1}, which is similar to those observed for hydrogen atom transfer (*7*). An outer-sphere electron transfer mechanism suggests a shallower distance dependence compared to that for atom transfer, so the guanine oxidation should be more prevalent under conditions where closely approaching the DNA is more difficult. Accordingly, we observe more guanine oxidation at low Mg^{2+} concentrations, where closely approaching $Pt_2(pop)_4^{4-}$ is inhibited by electrostatic repulsion. Thus, while relatively poor electronic coupling between guanine in DNA and nonintercalated oxidants leads to low adiabaticity in tunneling, this level of coupling is still much greater than that for atom transfer reactions, which require very a close approach of the oxidant to the activated C−H bond.

Although the results are consistent with an electron transfer mechanism, we have not detected 8-oxo-7,8-dihydroguanine, which is an excellent indicator of outer-sphere electron transfer (*39*−*44*), and certainly there are inner-sphere guanine oxidation mechanisms that could produce piperidine-labile scission (*4*, *14*, *38*). It is difficult to imagine an inner-sphere oxidation reaction of $Pt_2(pop)_4^{4-}$, since the complex does not have an activated oxygen atom and is not known to undergo any inner-sphere oxidation reactions (*7*). Further, such a reaction would have to exhibit a shallower distance dependence than the hydrogen transfer reaction to account for the observed Mg^{2+} concentration dependence. Nonetheless, we cannot definitively rule out alternative guanine oxidation mechanisms.

The guanine oxidation results for $Pt_2(pop)_4^{4-}$ parallel those for anthraquinones, which oxidize DNA by guanine electron transfer when intercalated but perform hydrogen abstraction when bound to the outside of the DNA near the sugar−phosphate backbone (*9*). The hydrogen abstraction pathway is only observed when the anthraquinone is bound close to the sugars, probably because the distance dependence for the hydrogen transfer pathway is much steeper than that for the electron transfer pathway and therefore requires close binding to the site of reaction. This effect has been exploited in studies of complexes based on $Rh(phen)_2(phi)^{3+}$, where the hydrogen transfer pathway has been used to map the binding site of the complex while in the same system where electron transfer has been observed at relatively long range (*10*). Likewise here, $Pt_2(pop)_4^{4-}$ performs guanine oxidation only when a close approach to the DNA sugar hydrogens is precluded by relatively low salt conditions or when less reactive RNA sugars are available.

ACKNOWLEDGMENT

We gratefully acknowledge the important role of Dr. S. A. Ciftan in developing our understanding of the nucleic acid cleavage chemistry of $Pt_2(pop)_4^{4-}$.

REFERENCES

1. Gold, L., Polisky, B., Uhlenbeck, O., and Yarus, M. (1995) *Annu. Rev. Biochem. 64*, 763−797.
2. Osborne, S. E., and Ellington, A. D. (1997) *Chem. Rev. 97*, 349−370.
3. Carter, P. J., Cheng, C.-C., and Thorp, H. H. (1996) *Inorg. Chem. 35*, 3348−3354.
4. Burrows, C. J., and Rokita, S. E. (1994) *Acc. Chem. Res. 27*, 295−301.
5. Chen, X., Burrows, C. J., and Rokita, S. E. (1992) *J. Am. Chem. Soc. 114*, 322−325.
6. Muller, J. G., Zheng, P., Rokita, S. E., and Burrows, C. J. (1996) *J. Am. Chem. Soc. 118*, 2320−2325.
7. Roundhill, D. M., Gray, H. B., and Che, C.-M. (1989) *Acc. Chem. Res. 22*, 55−61.
8. Breiner, K. M., Daugherty, M. A., Oas, T. G., and Thorp, H. H. (1995) *J. Am. Chem. Soc. 117*, 11673−11679.
9. Breslin, D. T., Coury, J. E., Anderson, J. R., McFail-Isom, L., Kan, Y., Williams, L. D., Bottomley, L. A., and Schuster, G. B. (1997) *J. Am. Chem. Soc. 119*, 5043−5044.
10. Hall, D. B., Holmlin, R. E., and Barton, J. K. (1996) *Nature 384*, 731−735.
11. Muller, J. G., Hickerson, R. P., Perez, R. J., and Burrows, C. J. (1997) *J. Am. Chem. Soc. 119*, 1501−1506.
12. Che, C. M., Butler, L. G., Grunthaner, P. J., and Gray, H. B. (1985) *Inorg. Chem. 24*, 4662.
13. Maniatis, T., Fritsch, E. F., and Sambrook, J. (1989) *Molecular Cloning: A Laboratory Manual*, 2nd ed., Cold Spring Harbor Laboratory Press, Plainview, NY.
14. Cheng, C.-C., Goll, J. G., Neyhart, G. A., Welch, T. W., Singh, P., and Thorp, H. H. (1995) *J. Am. Chem. Soc. 117*, 2970−2980.
15. Milligan, J. F., Groebe, D. R., Witherell, G. W., and Uhlenbeck, O. C. (1987) *Nucleic Acids Res. 15*, 8783−8798.
16. Bruce, A. G., and Uhlenbeck, O. C. (1978) *Nucleic Acids Res. 5*, 3665.
17. Peattie, D. A. (1979) *Proc. Natl. Acad. Sci. U.S.A. 76*, 1760−1764.
18. Stubbe, J., and Kozarich, J. W. (1987) *Chem. Rev. 87*, 1107.
19. Blommers, M. J. J., van de Ven, F. J. M., van der Marel, G. A., van Boom, J. H., and Hilbers, C. W. (1991) *Eur. J. Biochem. 201*, 33−51.
20. Kalsbeck, W. A., and Thorp, H. H. (1993) *J. Am. Chem. Soc. 115*, 7146−7151.
21. Steenken, S., and Jovanovic, S. V. (1997) *J. Am. Chem. Soc. 119*, 617−618.
22. Johnston, D. H., Cheng, C.-C., Campbell, K. J., and Thorp, H. H. (1994) *Inorg. Chem. 33*, 6388−6390.
23. Stemp, E. D. A., Arkin, M. R., and Barton, J. K. (1997) *J. Am. Chem. Soc. 119*, 2921−2925.
24. Saito, I., Takayama, M., Sugiyama, H., Nakatani, K., Tsuchida, A., and Yamamoto, M. (1995) *J. Am. Chem. Soc. 117*, 6406.
25. Henderson, P. T., Armitage, B., and Schuster, G. B. (1998) *Biochemistry 37*, 2991−3000.
26. Breslin, D. T., and Schuster, G. B. (1996) *J. Am. Chem. Soc. 118*, 2311−2319.
27. Cadet, J., Berger, M., Buchko, G. W., Joshi, P. C., Raoul, S., and Ravanat, J.-L. (1994) *J. Am. Chem. Soc. 116*, 7403−7404.
28. Johnston, D. H., Glasgow, K. C., and Thorp, H. H. (1995) *J. Am. Chem. Soc. 117*, 8933−8938.

29. Marciniak, R. A., Calnan, B. J., Frankel, A. D., and Sharp, P. A. (1990) *Cell 63*, 791−802.
30. Kao, S.-Y., Calman, A. F., Luciw, P. A., and Peterlin, B. M. (1987) *Nature 330*, 489−493.
31. Dingwall, C., Ernberg, I., Gait, M. J., Green, S. H., Heaphy, S., Karn, J., Lowe, A. D., Singh, M., and Skinner, M. A. (1990) *EMBO J. 9*, 4145−4153.
32. Carter, P. J., Cheng, C.-C., and Thorp, H. H. (1998) *J. Am. Chem. Soc. 120*, 632−642.
33. Neyhart, G. A., Cheng, C.-C., and Thorp, H. H. (1995) *J. Am. Chem. Soc. 117*, 1463−1471.
34. Kappen, L. S., and Goldberg, I. H. (1991) *Biochemistry 30*, 2034−2042.
35. Quigley, G. J., Teeter, M. M., and Rich, A. (1978) *J. Mol. Biol. 75*, 64.
36. Kalsbeck, W. A., Gingell, D. M., Malinsky, J. E., and Thorp, H. H. (1994) *Inorg. Chem. 33*, 3313−3316.
37. Pratviel, G., Bernadou, J., and Meunier, B. (1995) *Angew. Chem., Int. Ed. 34*, 746−769.
38. Neyhart, G. A., Grover, N., Smith, S. R., Kalsbeck, W. A., Fairley, T. A., Cory, M., and Thorp, H. H. (1993) *J. Am. Chem. Soc. 115*, 4423.
39. Arkin, M. R., Stemp, E. D. A., Pulver, S. C., and Barton, J. K. (1997) *Chem. Biol. 4*, 389−400.
40. Kasai, H., Yamgizumi, Z., Berger, M., and Cadet, J. (1992) *J. Am. Chem. Soc. 114*, 9692.
41. Spassky, A., and Angelov, D. (1997) *Biochemistry 36*, 6571−6576.
42. Muller, J. G., Duarte, V., Hickerson, R. P., and Burrows, C. J. (1998) *Nucleic Acids Res. 26*, 2247−2249.
43. Cullis, P. M., Malone, M. E., and Merson-Davies, L. A. (1996) *J. Am. Chem. Soc. 118*, 2775−2781.

BI981479Z